DOI: 10.21062/mft.2026.027 http://www.journalmt.com

Marker-Based Photogrammetric Modelling of the Lower Leg Using Agisoft Metashape for 3D-Printed Splints

Minh-Ky Nguyen (0000-0001-7445-3078)[1], Natasa Naprstkova (0000-0003-4433-0581)[2], Tuong Nguyen Van (0000-0002-6238-5458)[3]
[1]Faculty of Mechanical Engineering, Ho Chi Minh City University of Technology and Engineering. 01 Vo Van Ngan, Thu Duc Ward, Ho Chi Minh City, Viet Nam. Email: kynm@hcmute.edu.vn
[2]Faculty of Mechanical Engineering, University of Jan Evangelista in Ústí nad Labem. Pasteurova 3334/7, 400 01 Usti nad Labem, Czech Republic. E-mail: natasa.naprstkova@ujep.cz
[3]Faculty of Mechanical Engineering, Nha Trang University. 02 Nguyen Dinh Chieu, Nha Trang, Viet Nam. E-mail: tuongnv@ntu.edu.vn (corresponding author)

Designing patient-specific 3D-printed splints requires accurate limb geometry acquisition. Professional 3D scanners are commonly used for acquiring the 3D geometry of limbs, but they are high-cost and less accessible in routine clinical practice. Photogrammetry, which reconstructs 3D models from 2D images captured by digital or smartphone cameras, provides a low-cost and flexible alternative. This study proposes a practical workflow for lower leg modelling using Agisoft Metashape and AutoCAD, employing two printed markers as scaling references. The two markers with a precisely defined inter-marker distance of 150 mm were printed on an A4 sheet and used as reference objects to scale the photogrammetric model to real-world size. The accuracy of the photogrammetric model was evaluated in GOM Inspect by comparing it with a reference scanned model. The results showed that the photogrammetric model has an average deviation of −0.59 mm. Additionally, a physical fit evaluation with a 3D-printed splint further confirmed good conformity between the splint and the lower leg. The findings show that the accuracy of inter-marker distance plays a critical role in photogrammetric scaling.

Keywords: Photogrammetry, 3D-printed splint, Marker-based scaling, Lower leg

1 Introduction

Plaster and fiberglass casts have traditionally been used to treat cracks or fractures of the forearm, wrist, elbow, lower leg, ankle, and related anatomical regions. However, these conventional casts have a number of disadvantages, such as being heavy and uncomfortable, pruritus, and skin irritation when exposed to moisture [1-3]. Because of these limitations, 3D-printed splints have recently been introduced as alternatives to conventional ones. These splints offer a custom fit, high strength, low weight, enhanced aesthetics, a wide range of colours, reduced skin irritation, and a removable design, thereby significantly enhancing patient comfort [3-6].

In order to fabricate a 3D-printed splint, the first step is to digitise the limbs using a reverse engineering process [7-10]. The acquired data consist of a three-dimensional (3D) point cloud, which is subsequently processed using reverse engineering software and serves as the input data for splint design. In most cases, limb digitisation is performed using 3D scanners [7,9,10]. Although these devices are capable of capturing high geometric accuracy, they are not frequently available in many hospitals due to their high cost and the fact that they are prohibitively expensive.

In addition to professional digitisation equipment, limb data acquisition can also be performed using a digital camera or a smartphone camera [1,2,11-15]. In such cases, photogrammetry software is employed to reconstruct a photogrammetric 3D model from a set of 2D photos. Tuong et. al. effectively reconstructed 3D arm models with adequate geometric accuracy for the purpose of designing and fabricating patient-specific 3D printed arm splints [1,2]. In this study, they took pictures of arms using a smartphone camera, reconstructed photogrammetric models with Agisoft Metashape (Agisoft LLC, Russia), and subsequently scaled the models in CATIA (Dassault Systèmes, France) [1,2]. Although the integration of CATIA can enable a more controlled scaling procedure and improve dimensional consistency of the photogrammetric model, the use of CATIA significantly increases software cost and operational complexity. Because CATIA is a high-end industrial CAD system, its application in biomedical photogrammetry requires well-trained mechanical engineers and expensive licenses, which limit the accessibility, scalability, and clinical applicability of the proposed workflow. Replacing CATIA with

a low-cost CAD system can significantly reduce software costs and lower the technical barrier for users, thereby enhancing the accessibility and practical applicability of photogrammetry in the design and fabrication of 3D-printed casts. This paper presents a lower-leg modelling method based on photogrammetry using Agisoft Metashape and AutoCAD (Autodesk, USA), which can be applied to the low-cost design and fabrication of 3D-printed leg splints, effectively overcoming the cost and skill barriers associated with the use of high-end CAD software.

2 Methods

2.1 Image acquisition setup

In this study, an Olympus Stylus 7030 digital camera was used to capture images of the volunteer's lower leg. The camera has a resolution of 14 megapixels, an ISO range of 64–1600, and an autofocus function. The low ISO capability of the camera is consistent with the image acquisition recommendations of Agisoft Metashape [16]. In order to supply sufficient illumination when taking photos, a 55 W LED ring light was employed.

The output model generated by Agisoft Metashape is an unscaled 3D model, which is not suitable for lower-leg splint modelling and design tasks. Therefore, this model needs to be scaled to match its real-world size, ensuring consistency between the reconstructed 3D geometry and the anatomical dimensions required for modelling of 3D-printed lower-leg splints. Coded targets in Agisoft Metashape enable the establishment of a coordinate system, control of model scaling, and reduction of reconstruction errors during the 3D reconstruction process [16]. The coded targets can be directly printed from Agisoft Metashape and placed on or adjacent to the target object during image acquisition [15,18,19]. Measured with handheld tools, the distance between the targets can be employed for scaling purposes in order to translate the photogrammetric model to dimensions that are more representative of the real world. The accuracy of the photogrammetric model is directly dependent on the precision of the target distance measurement. To further improve the accuracy of the photogrammetric model, this study employed a sheet of paper containing two reference markers, which was placed adjacent to the lower leg during image acquisition. The reference markers were obtained from the Agisoft Metashape library, were redrawn in AutoCAD, and printed on an A4 sheet at a 100% scale. When scaling the model to its actual size, the scaling factor was determined using the 150 mm distance between the two reference markers.

The volunteer was a 22-year-old Vietnamese male with a body weight of 54 kg. In order to minimize background noise while taking pictures, the volunteer stood on a floor covered in black fabric. The lower leg to be captured was kept in an upright position, while the other was flexed. During image acquisition, the photographer held the LED light in one hand and the camera in the other hand. The camera was configured with an ISO setting of 64, which is the minimum value. The distance between the camera and the lower leg was approximately 350–400 mm. During image acquisition, the lower leg was photographed from different viewpoints as the photographer moved around the volunteer, and consecutive images were captured with an overlap of approximately 60–80% [16]. The Fig. 1 shows the Arrangement of image acquisition.

Fig. 1 *Arrangement of image acquisition*

2.1 Photogrammetric reconstruction

Agisoft Metashape enables image-based 3D surface reconstruction through a structured multi-stage processing pipeline [16]. In the first stage, the acquired images were imported and aligned to estimate camera poses, resulting in the generation of a sparse point cloud. In this stage, the two reference markers were detected. The first step was followed by dense point cloud reconstruction based on the estimated camera parameters and image data, which may be refined prior to surface reconstruction. Subsequently, a polygonal mesh representing the object surface is generated from the dense point cloud, with optional texture mapping applied when required. Before building the texture model, the mesh model of the lower leg was scaled to the actual dimensions of the subject using the distance between the two targets as a scaling parameter. In the final stage, the reconstructed mesh is exported in a neutral file format to facilitate subsequent processing. The STL (Standard Tessellation Language) file format was used as input data for lower-leg splint modelling in a CAD

environment. A workstation (3.7 GHz CPU, 16 GB RAM, 8 GB GPU) was used for image processing.

2.2 Accuracy evaluation

Immediately after image acquisition, the lower leg was scanned using a CR-Scan 01 handheld 3D scanner (Reality, China), which provides a nominal accuracy of 0.1 mm. The leg posture during scanning was identical to that used during image acquisition, with a scanning distance of approximately 0.5 to 0.6 m. The scanning process was performed under illumination provided by overhead fluorescent ceiling lights. CR Studio software was used to automatically create the 3D model of the lower leg. After that, the scanned model was exported in STL format.

The geometric accuracy of the photogrammetric model was evaluated by comparing it with the scanned model using GOM Inspect 2017 (Zeiss Group, Germany), which enables dimensional inspection and comparison of two STL files. In order to show spatial differences between the two models, the findings were displayed both statistically and as a colour-coded deviation map [20-23].

2.3 Physical fit evaluation

In addition to virtual verification, a physical 3D-printed splint was fabricated to evaluate the fitting performance of the splint on the target lower leg. For this purpose, the photogrammetric lower-leg model was used as the reference geometry for designing the splints in Creo Parametric. The splint was manufactured using a low-cost 3D printer with polylactic acid (PLA) material. Following printing and post-processing, the inner surface of the 3D-printed splint was uniformly covered with a thin layer of coloured powder. The volunteer then wore the 3D-printed splint for one hour. This duration could be enough for the powder on the splint to adhere to the skin and for observing the gap between the inner surface of the splint and the limb [1]. Subsequently a visual colour-based inspection was performed to assess the contact uniformity and overall fit between the splint and the lower leg.

3 Application and discussion

93 pictures, ranging in size from 349 KB to 449 KB, were taken. In Agisoft Metashape, after completing the point cloud generation process, the Detect Markers tool was used to identify the reference markers named target 1 and target 2 (Fig. 2a). Following noise removal, a dense point cloud and a polygonal mesh model were generated, as shown in Fig. 2b. Prior to constructing the complete lower-leg model, the polygonal mesh of the lower leg was scaled to match the real-world dimensions of the subject's lower leg. The Create Scale Bar tool was employed to define a reference distance of 150 mm between the two targets. After scaling the model to real-world dimensions, texture generation was performed. Once the 3D lower-leg model had been scaled to its actual size, the markers were removed, and the 3D model was trimmed, as illustrated in Fig. 2c. The marker removal step preserved the established scaling and did not affect the adjusted model dimensions. The automatic processing time in Agisoft Metashape took roughly 20 minutes, whereas noise removal took almost 1.5 hours.

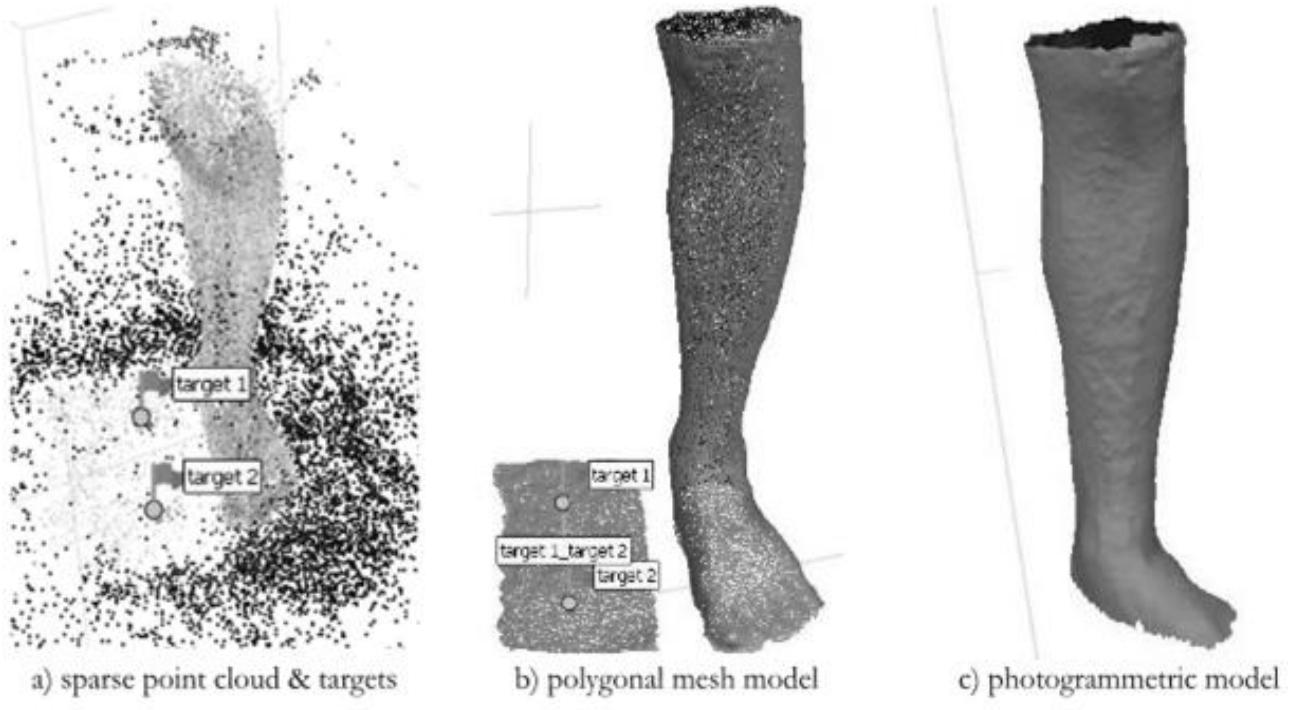

Fig. 2 *Different stages of image processing*

For the purpose of virtual accuracy assessment, the scanned reference model and the photogrammetric model were imported into GOM Inspect, where automatic alignment was performed prior to quantitative comparison. The deviation comparison was performed on the region below the knee and above the ankle, which was assumed to be the area immobilized by a 3D-printed splint. Fig. 3 illustrates the resulting colour-coded deviation map together with selected numerical deviation values between the two STL files.

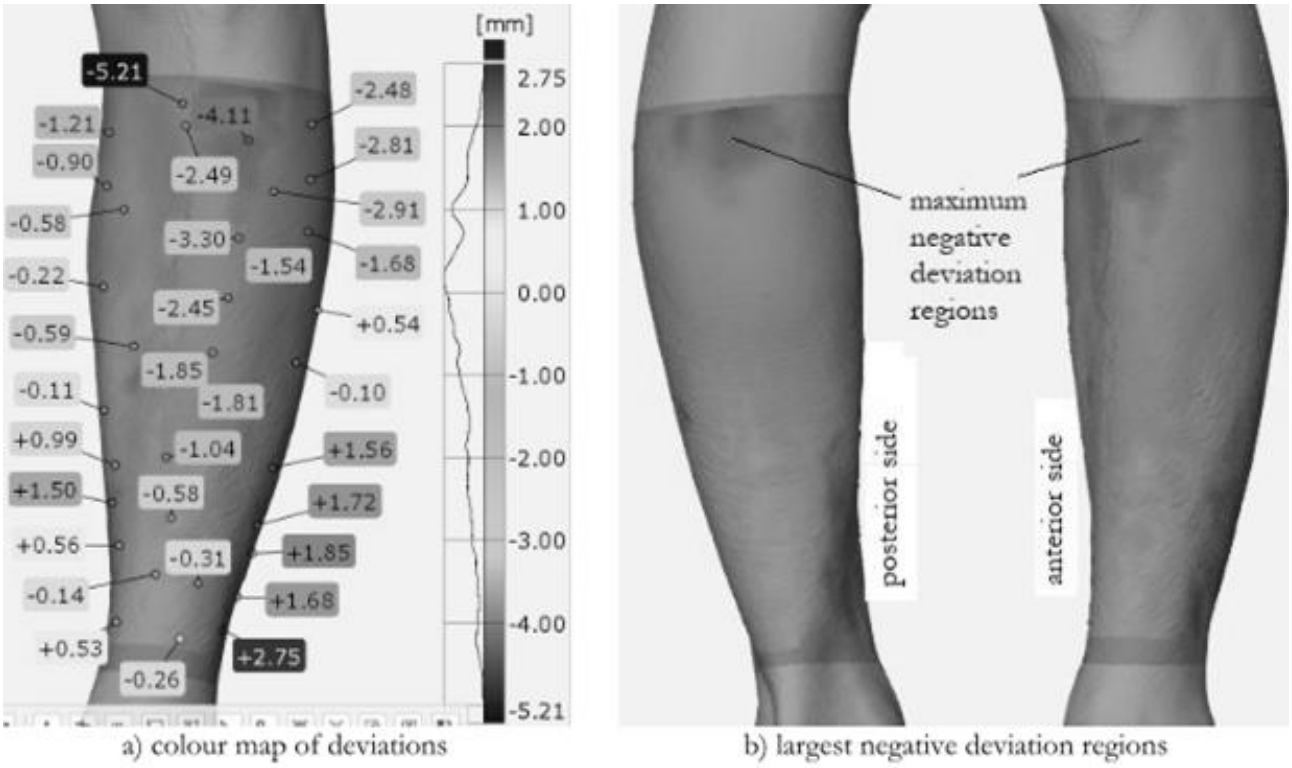

Fig. 3 *Colour map of deviations and regions of largest negative deviations, for a) Minimum deviation: -5.21 mm, Maximum deviation: +2.75 mm, Arithmetic mean deviation: -0.59 mm, Standard deviation: 1.57 mm*

From Fig. 3a, it can be observed that deviations occur over the entire surface of the photogrammetric model compared with the scanned model. The green, light green, and yellow regions indicate that the photogrammetric model is larger than the scanned model, whereas the blue regions represent negative deviations of the photogrammetric model relative to the scanned model. The maximum positive deviation, maximum negative deviation, and mean deviation were +2.75 mm, −5.21 mm, and −0.59 mm, respectively, with a standard deviation of 1.57 mm. As shown in Fig. 3b, the largest negative deviations are mainly observed in the regions below the knee on both the posterior and anterior sides of the lower leg. These deviations could be primarily caused by soft tissue deformation and muscle contraction induced by the single-leg standing posture, in which the measured leg bears the full body weight. Maintaining balance in this posture induces continuous and asymmetric muscle contraction, leading to temporal variations in the surface shape of the lower leg throughout the image capture process. In addition, there are unfavourable geometric characteristics for photogrammetry on the sub-knee regions, such as rapidly changing curvature, limited surface texture, and specular reflections. These factors can cause negative effects on feature matching and dense point cloud reconstruction, in the end, causing surface shrinkage and large negative deviations in the photogrammetric model created in Agisoft Metashape.

In general, the discrepancies between the two models may be attributed to leg movement during image acquisition or prolonged posture maintenance, which can promote muscle expansion, resulting in variances between the leg state during photography and during scanning. Besides, deviations in the photogrammetric model may arise from errors in creating the two reference markers in AutoCAD and in printing them on the A4 sheet. Since the distance between the two markers is employed as the scaling parameter, which can amplify the propagated error, errors in creating these markers could be the main cause of the deviations between the two models.

The negative mean deviation indicates that the photogrammetric model is slightly smaller than the scanned model on average, while the standard deviation of 1.57 mm suggests that the differences

between the two models are within the range of -2.16 mm and +0.98 mm. It is evident from the deviation colour map that, in comparison to the rest of the model, areas with significant deviations comprise a comparatively small area. Most of the differences between the two models are within ±1 mm. The average deviation between the two models is −0.59 mm. Table 1 compares the average deviations of photogrammetric models in human body reconstruction reported in some recent studies that used various types of reference objects for image acquisition and Agisoft Metashape for image processing.

Tab. 1 *Average deviations of photogrammetric models in human body reconstruction*

Studies	Photogrammetric model	Image acquisition device	Reference object	Average deviation (mm)
This study	Lower leg (man)	Olympus Stylus 7030 digital camera	An A4 paper with 2 markers	−0.59
Tuong & Natasa [1]	Forearm (woman)	Samsung Galaxy S10 Plus smartphone	A cylinder	−0.04
	wrist-hand (woman)			−0.45
	Forearm (male)			+0.31
	wrist-hand (man)			−0.04
Tuong et al. [2], [24]	Forearm part (man)	Samsung Galaxy S10 Plus smartphone	A cylinder	+0.22
Salvador et al. [11]	Rubber clubfoots	Raspberry Pi camera module	4 markers on an acrylic bar	−0.7129÷+0.4147
Tursi et al. [13]	Lower leg	iPhone 6S smartphone	Markers taped to the lower leg	+2.0
Quispe-Enriquez et al. [25]	Head volunteers	Samsung Galaxy S22 smartphone	A coded cap	+0.58÷+1.59

In general, compared with previous studies, the average deviation achieved in this study is comparable to or lower than most reported values. This study used two coded markers printed on an A4 paper with an inter-marker distance of 150 mm, which was precisely created using AutoCAD. This distance was used as the scaling reference and the average deviation between the two CAD models is −0.59 mm. Tuong and Natasa reported average deviations between −0.45 mm and +0.31 mm for forearm and wrist–hand models [1], while Tuong et al. achieved +0.22 mm for a male forearm [2,24]. It can be seen that using a cylinder as the scaling object could yield photogrammetric models with better accuracy. It should be noted that the diameter of the cylinder can be accurately measured with small tools such as vernier callipers or micrometres, however, CATIA has been used for scaling purposes [1,2]. Salvador et al. utilised four markers engraved on an acrylic bar and reported average deviations from −0.7129 mm to −0.4147 mm [11]. Salvador's method can ensure a precise distance between markers, and reduce scaling-related error propagation. This explains the consistently low average deviations reported; however, the imaging hardware is quite complicated. In the study of Tursi et al. [13], markers were taped to the lower leg. This method led to an average deviation of approximately +2.0 mm, which is rather big compared to that of other studies. This larger deviation can be attributed to several factors, including uncertainty in measuring the distance between markers on the limb with handheld instruments. This situation is also reflected in the study by Quispe-Enriquez et al. [25], where a specially coded cap was used for modelling photogrammetric models of human heads, resulting in bigger average deviations, from +0.58 mm to +1.59 mm.

Generally, the dimensional parameter employed to scale the photogrammetric model to its actual size is a significant factor influencing the accuracy of the model. Rigid reference objects, such as a cylinder or a bar with engraved markers geometry can provide superior control over scaling accuracy. Nevertheless, our study demonstrates that even a simple printed-marker setup can achieve competitive accuracy, without using high-end CAD software. This finding is particularly relevant for practical biomedical applications, where low-cost and adaptable reference objects are often preferred.

For the fit evaluation, the photogrammetric model was used as the reference geometry to design a splint in Creo Parametric (PTC, USA). The outer surface of the photogrammetric model was used as the inner surface of the splint model, resulting in no gap between the splint and the limb. In practical splint design, an additional offset is typically introduced to improve wearing comfort. Figure 4 presents the fit-checking results, showing that the contact colour

patterns on the limb are continuous and uniformly distributed, indicating good conformity between the splint and the limb. These findings align with the CAD model comparison results mentioned above. Overall, the fit evaluation shows that the photogrammetric model produced using the proposed method can have sufficient accuracy to be used as a reference for 3D-printed splint design.

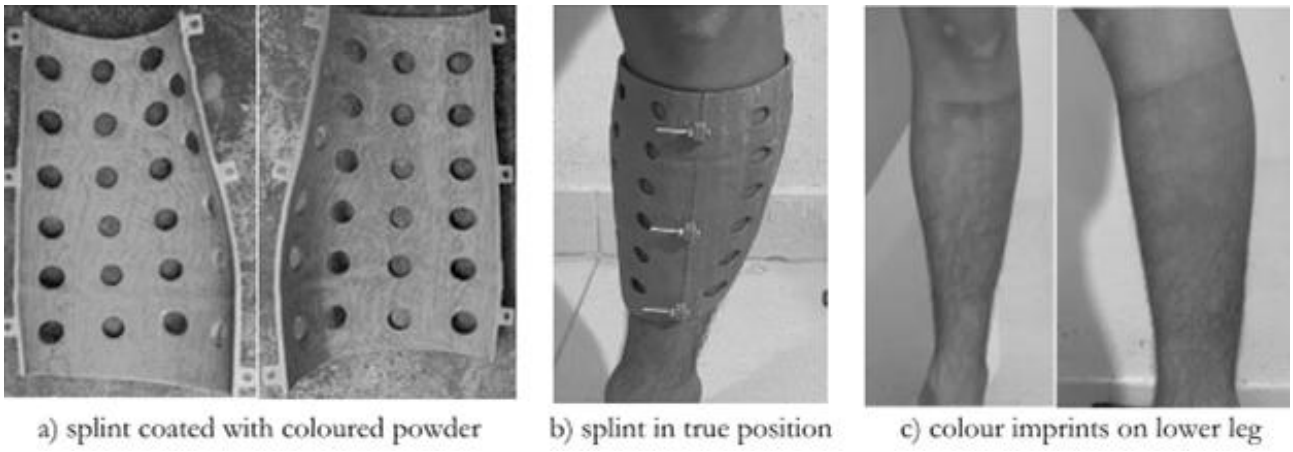

Fig. 4 *3D printed splint and the colour imprints on the lower leg*

The accuracy of human limb models reconstructed using Agisoft Metashape can depend on various factors such as image quality, lighting conditions, limb posture, skin characteristics, and the use of reference objects, … [1,2,14]. When considering only the use of reference objects, this study suggested a simple way by using two coded markers with a known distance created in AutoCAD and printed on an A4 sheet. This approach eliminates the inconsistency observed in previous studies that used low-cost data acquisition devices (smartphones) while relying on expensive CAD software (CATIA) to obtain proper photogrammetric models [1,2]. Replacing CATIA with a low-cost CAD system can significantly reduce costs and lower the technical barrier for users, thereby enhancing the accessibility and practical applicability of photogrammetry in the design and fabrication of 3D-printed lower leg splints. Additional cases involving adult subjects were also examined and produced results consistent with those reported in this paper. These findings suggest that photogrammetric models generated using the proposed approach achieve an adequate level of accuracy and could be used as reliable reference models for modelling 3D printed splints.

4 Conclusion

In order to design and manufacture customised 3D-printed splints, this study suggested a low-cost approach for lower-leg modelling using Agisoft Metashape and AutoCAD. Without using high-end CAD software, the reconstructed model was successfully scaled to real-world sizes by employing two printed markers on an A4 sheet as scaling references. In GOM Inspect, a quantitative comparison with a reference scanned model showed an average deviation of −0.59 mm, which is comparable to or lower than most values reported in previous human body reconstruction studies. The results confirm that the accuracy of the inter-marker distance can play an important factor influencing overall model accuracy. Furthermore, physical fit evaluation using a 3D-printed splint confirmed good conformity between the splint and the limb. The results of the virtual accuracy assessment and physical test show that the photogrammetric model has a size similar to that of the subject's lower leg. This model can be used as the reference model for the process of design and manufacture of 3D-printed lower leg splints. Overall, the proposed method shows great promise for practical applications, especially in environments with limited resources where affordability, accessibility, and enough geometric accuracy are crucial. Future work will concentrate on investigating the influence of different marker configurations and inter-marker distances on scaling accuracy, as well as extending the proposed workflow to other anatomical regions and clinical scenarios.

Acknowledgement

The work of this paper is supported by Ho Chi Minh City University of Technology and Engineering and Nha Trang University, Viet Nam.

References

[1] VAN, T. N. & NAPRSTKOVA, N. (2024). Accuracy of Photogrammetric Models for 3D Printed Wrist-hand Orthoses. In: *Manufacturing Technology*, Vol. 24, No. 3, p. 458-464. J. E.

Purkyně University in Usti nad Labem, Czech Republic. ISSN 1213-2489

[2] VAN, T. N., LE THANH, T., VAN, T. N., NAPRSTKOVA, N. (2023). Smartphone-based Data Acquisition Method for Modelling 3D Printed Arm Casts. In: *Manufacturing Technology*, Vol. 23, No. 2, pp. 260-267. J. E. Purkyně University in Usti nad Labem, Czech Republic. ISSN 1213-2489

[3] VAN LIESHOUT, E. M. M., VERHOFSTAD, M. H. J., BEENS, L. M., VAN BEKKUM, J. J. J., WILLEMSEN, F., JANZING, H. M. J., & VAN VLEDDER, M. G. (2022). Personalized 3D-printed Forearm Braces as an Alternative for a Traditional Plaster Cast or Splint; A Systematic Review. In: *Injury*, Vol. 53 Suppl. 3, pp. S47–S52. Elsevier, Amsterdam, Netherlands. ISSN 0020-1383

[4] SCHWARTZ, D.A., SCHOFIELD, K.A. (2025). Utilization of 3D Printed Orthoses for Musculoskeletal Conditions of the Upper Extremity: A Systematic Review. In: *Journal of Hand Therapy*, Vol. 36, No. 1, pp. 166-178. Elsevier, Amsterdam, Netherlands. ISSN 0894-1130

[5] XU, C., WANG, L., ZHANG, M., LI, X., & LI, K. (2025). A Clinical Study on the Application of Three-Dimensionally Printed Splints Combined with Finite Element Analysis in Paediatric Distal Radius Fractures. In: *Frontiers Pediatrics*, Vol. 13, 1559762. Frontiers, Lausanne, Switzerland. ISSN 2296-2360

[6] GLAZER, C., ORAVITAN, M., PANTEA, C., STANILA, A. M., JURJIU, N. A., TOTOK, A., MARGHITAS, M. P., AVRAM, C. (2025). 3D-printed Orthoses vs. Traditional Plaster Cast: A Compara-Tive Clinical Study. In: *Balneo and PRM Research Journal*, Vol. 16, No. 1, p. 785. Romanian Association of Balneology, Bucharest, Romania. ISSN 2734-8458

[7] KELLER, M., GUEBELI, A., THIERINGER, F., HONIGMANN, P. (2021). In-hospital Professional Production of Patient-specific 3D-printed Devices for Hand and Wrist Rehabilitation. In: *Hand Surgery Rehabilitation*, Vol. 40, No. 2, pp. 126-133. Elsevier, Amsterdam, The Netherlands. ISSN 2468-1210

[8] LAZZERI, S., TALANTI, E., BASCIANO, S., BARBATO, R., FONTANELLI, F., UCCHEDDU, F., SERVI, M., VOLPE, Y., VAGNOLI, L., AMORE, E., MARZOLA, A., MCGREEVY, K. S., CARFAGNI, M. (2022). 3D-Printed Patient-Specific Casts for the Distal Radius in Children: Outcome and Pre-Market Survey. In: *Materials*, Vol. 15, No. 8, 2863. MDPI, Basel, Switzerland. ISSN 1996-1944

[9] POPESCU, D., BACIU, F., VLĂSCEANU, D., MARINESCU, R., LĂPTOIU, D. (2023). Investigations on the Fatigue Behaviour of 3D-Printed and Thermoformed Polylactic Acid Wrist–Hand Orthoses. In: *Polymers*, Vol. 15, NO. 12, 2737. MDPI, Basel, Switzerland. ISSN 2073-4360

[10] JAN, Z., ABAS, M., KHAN, I., QAZI, M. I., USMAN JAN, Q. M. (2023). Design and Analysis of Wrist Hand Orthosis for Carpal Tunnel Syndrome using Additive Manufacturing, In: *Journal of Engineering Research*, Vol. 12, 001. Elsevier, Amsterdam, The Netherlands. ISSN 2307-1877

[11] SALVADOR, T., SLAGLE, J., CHAPRNKA, G., AGRONIN, M, OETGEN, M., TABAIE, S., CLEARY, K, DAYAL, A., Development of a Novel Photogrammetry Method for Acquiring 3D Surface Models of Infant Clubfoot Anatomy. In: *Medical Imaging 2022: Image-Guided Procedures, Robotic Interventions, and Modelling*, Vol. 12034, 120342E-3. SPIE, Washington USA. ISBN 9781510649446

[12] HERNANDEZ, A., LEMAIRE, E. (2017). A Smartphone Photogrammetry Method for Digitising Prosthetic Socket Interiors. In: *Prosthetics and Orthotics International*, Vol. 41, No. 2, pp. 210–214. SAGE Publications, California, United States. ISSN 1746-1553

[13] TURSI, A., KURILLO, G., BAJCSY, R. (2017). Automatic Detection of Body Landmarks in Human Body Scans - Lower Limb Analysis for Biomedical and Footwear Applications. In: *The 8th International Conference and Exhibition on 3D Body Scanning and Processing Technologies*, pp. 179-191. Montreal QC, Canada. ISBN 978-3-033-06436-2

[14] OLIVIER, M. (2019). *A Low-Cost Custom Knee Brace via Smartphone Photogrammetry*. Master thesis, University of Ottawa. Ottawa, Canada

[15] WALTERS, S., METCALFE, B., TWISTE, M., SEMINATI, E., BAILEY, N. Y. (2024). Smartphone Scanning is a Reliable and Accurate Alternative to Contemporary Residual Limb Measurement Techniques. In: *PLOS ONE*, Vol. 19, No. 12, e0313542, ISSN 1932-6203

[16] AGISOFT LLC. (2025). Agisoft Metashape User Manual Professional Edition, version 2.3. Agisoft LLC.

[17] PAVELKA, K., GREŠLA, O. (2025). The Use of Close-range Photogrammetry and 3D Scanning for Diagnostic Purposes in Mechanical Engineering, In: *The International Archives of the Photogrammetry, Remote Sensing and Spatial Information Sciences*, Vol. XLVIII-5/W3, pp. 77-82, Tashkent, Uzbekistan. ISSN-L: 2194-9034

[18] FARZAD, M., MACDERMID, J., FERREIRA, L., TUTUNEA-FATAN, O. R., SAEEDI, M., GORSKI, A., BALAJI, A., CUYPERS, S. (2025). Development of a Web-based Application for Initial Hand Evaluation and 3D Scanning: A Pilot Feasibility and Validity Study. In: *Journal of Hand Therapy*, Vol. 38, No. 2, pp. 318-327. Elsevier, Amsterdam, The Netherlands. ISSN 0894-1130,

[19] TEIXEIRA COELHO, L. C., PINHO, M. F. C., MARTINEZ DE CARVALHO, F., MENEGUCI MOREIRA FRANCO, A. L., QUISPE-ENRIQUEZ, O. C., ALTÓNAGA, F. A., & LERMA, J. L. (2025). Evaluating the Accuracy of Smartphone-Based Photogrammetry and Videogrammetry in Facial Asymmetry Measurement. In: *Symmetry*, Vol. *17, No.* 3, 376. MDPI, Basel, Switzerland. ISSN 2073-8994

[20] TUONG, N.V. (2018), Manufacturing Method of Spiral Bevel Gears Based on CAD/CAM and 3-Axis Machining Center. In: *MM Science Journal*, Vol. June 2018, pp. 2401-2405. MM Publishing, Czech Republic. ISSN 1803-1269

[21] VAN, T.N., LE THANH, T., NAPRSTKOVA, N. (2021). Measuring propeller pitch based on photogrammetry and CAD. In: *Manufacturing Technology*, Vol. 21, No. 5, pp.706-713. J. E. Purkyně University in Usti nad Labem, Czech Republic. ISSN 1213-2489

[22] SEDLAK, J., HRUSECKA, D., CHROMJAKOVA, F., MAJERIK, J. & BARENYI, I. (2021). Analysis of the Wear on Machined Groove Profiles Using Reverse Engineering Technology. In: *Manufacturing Technology*, Vol. 21, No. 4, pp. 529-38. J. E. Purkyně University in Usti nad Labem, Czech Republic. ISSN 1213-2489

[23] FABIAN, M., HUŇADY, R. & KUPEC, F. (2022). Reverse Engineering and Rapid Prototyping in the Process of Developing Prototypes of Automotive Parts. In: *Manufacturing Technology*, Vol. 22, No. 6, pp. 669-78. J. E. Purkyně University in Usti nad Labem, Czech Republic. ISSN 1213-2489

[24] TUONG N. V. (2023). Design and Manufacture 3D Printed Arm Cast from Data Taken by Smartphone. Research report, Nha Trang University, Viet Nam

[25] QUISPE-ENRIQUEZ, O. C., VALERO-LANZUELA, J. J., LERMA, J. L. (2024). Craniofacial 3D Morphometric Analysis with Smartphone-Based Photogrammetry. In: *Sensors* 2024, Vol. 24, No. 1, 230. MDPI, Basel, Switzerland. ISSN 1424-8220